Published in final edited form as:
J Immunol. 2013 February 15; 190(4): 1859–1872. doi:10.4049/jimmunol.1201725.

Activation of Toll-Like Receptor 4 Is Required for the Synergistic Induction of Dual Oxidase 2 and Dual Oxidase A2 by Interferon-γ and Lipopolysaccharide in Human Pancreatic Cancer Cell Lines[§]

Yongzhong Wu[*], **Jiamo Lu**[*], **Smitha Antony**[*], **Agnes Juhasz**[*], **Han Liu**[†], **Guojian Jiang**[*], **Jennifer L. Meitzler**[*], **Melinda Hollingshead**[†], **Diana C. Haines**[‡], **Donna Butcher**[‡], **Krishnendu Roy**[†], and **James H. Doroshow**[*,†]

[*]Laboratory of Molecular Pharmacology of the Center for Cancer Research, National Cancer Institute, National Institutes of Health, Bethesda, MD 20892

[†]Division of Cancer Treatment and Diagnosis, National Cancer Institute, National Institutes of Health, Bethesda, MD 20892

[‡]Pathology/Histotechnology Laboratory, SAIC Frederick, Inc./Frederick National Laboratory for Cancer Research, National Cancer Institute, Frederick, MD 21702

Abstract

Pancreatitis is associated with release of pro-inflammatory cytokines and reactive oxygen species and plays an important role in the development of pancreatic cancer. We recently demonstrated that dual oxidase 2 (Duox2), an NADPH oxidase essential for ROS-related, gastrointestinal host defense, is regulated by IFN-γ-mediated Stat1 binding to the Duox2 promoter in pancreatic tumor lines. Because lipopolysaccharide (LPS) enhances the development and invasiveness of pancreatic cancer in vivo following Toll-like receptor 4 (TLR4)-related activation of NF-κB, we examined whether LPS, alone or combined with IFN-γ, regulated Duox2. We found that upregulation of TLR4 by IFN-γ in BxPC-3 and CFPAC-1 pancreatic cancer cells was augmented by LPS, resulting in activation of NF-κB, accumulation of NF-κB (p65) in the nucleus, and increased binding of p65 to the Duox2 promoter. TLR4 silencing with siRNAs, and two independent NF-κB inhibitors, attenuated LPS- and IFN-γ–mediated Duox2 upregulation in BxPC-3 cells. Induction of Duox2 expression by IFN-γ and LPS may result from IFN-γ-related activation of Stat1, acting in concert with NF-κB-related upregulation of Duox2. Sustained extracellular accumulation of H_2O_2 generated by exposure to both LPS and IFN-γ was responsible for an ≈ 50% decrease in BxPC-3 cell proliferation associated with a G_1 cell cycle block, apoptosis, and DNA damage. We also demonstrated up-regulation of Duox expression in vivo, in pancreatic cancer xenografts and in patients with chronic pancreatitis. These results suggest that inflammatory cytokines can interact to produce a Duox-dependent pro-oxidant milieu that could increase the pathologic potential of pancreatic inflammation and pancreatic cancer cells.

Introduction

A substantial body of evidence suggests that chronic inflammation of the pancreas plays an important role in the subsequent development of pancreatic cancer, and that the pathogenesis of exocrine cancers of the pancreas may be intimately related to the release of pro-

Address correspondence to: James H. Doroshow, MD, Bldg. 31, Room 3A-44, 31 Center Drive, National Cancer Institute, NIH, Bethesda, MD 20892. Fax: 301-496-0826; doroshoj@mail.nih.gov.

[§]Abbreviations used in this article: ROS, reactive oxygen species; Duox2, dual oxidase 2; DuoxA2, dual oxidase maturation factor 2; Nox, NADPH oxidase; TLR4, Toll-like receptor 4; siRNA, small interfering RNA; LPS, lipopolysaccharide

inflammatory cytokines and cytokine-related reactive oxygen formation (1-4). Recently, the role of repetitive bouts of asymptomatic pancreatic inflammation in tumor development has been emphasized, as well as the critical role of anti-inflammatory interventions to enhance the repair of inflammation-related tissue injury and reduce subsequent tumorigenesis (5). Pancreatic cancer cells have been demonstrated to produce reactive oxygen species (ROS) in a growth factor-dependent fashion, and these reactive species play an important role in the proliferative capacity of these cells (6-8). It is possible, therefore, that during repeated bouts of pancreatitis, cytokine-related ROS production could increase genetic instability (9,10), while decreasing the tumor suppressor functions of essential protein phosphatases (11), thus enhancing the possibility of malignant transformation.

While it has been known for over two decades that tumor cells can produce a significant flux of H_2O_2 (12), only more recently has it become clear that much of the reactive oxygen formation emanating from human tumors may originate from members of the recently-described family of epithelial NADPH oxidases (reduced nicotinamide adenine dinucleotide phosphate oxidases [Noxs]) (13,14). Dual oxidase 2 (Duox2) is one of the seven members of the Nox gene family; although originally described as an H_2O_2-producing enzyme in the thyroid that plays a critical role in thyroid hormone biosynthesis (15), Duox2 has also been found in bronchial epithelium and throughout the gastrointestinal tract (16,17). In airway mucosal cells, Duox2 plays an important role in the generation of H_2O_2 for host defense against a variety of pathogens (18-20); under the stress induced by an infectious agent, Duox2 expression is regulated by several inflammatory stimuli, including IFN-γ, flagellin, and rhinovirus (16,20). Duox2-induced ROS also appear to play a role in the antibacterial response in the gut (21,22). However, the expression of Duox2 is significantly increased in human colon biopsies, and in isolated intestinal epithelial cells, from patients with inflammatory bowel disease (both Crohn's disease and ulcerative colitis) compared to healthy control subjects (21,23), suggesting that an unchecked ROS response to pathogens could contribute to the tissue injury observed in these chronic inflammatory disorders.

Previous work from our laboratory has revealed that the pro-inflammatory cytokine IFN-γ initiates a Duox2-induced ROS cascade in human pancreatic cancer cells (24). Several recent studies have demonstrated, furthermore, that pro-inflammatory components of the bacterial cell wall, including lipopolysaccharide (LPS), mediate Nox-dependent ROS generation during the inflammatory response in the airway and gastrointestinal tract, in part due to direct interactions between members of the Nox family and Toll-like receptor 4 (TLR4), the critical downstream target that recognizes LPS from Gram-negative bacteria (25,26). TLR4-related signaling has recently been suggested to play a role in the pathogenesis of acute pancreatitis in model systems as well as in the clinic (27-29). Because LPS-related TL4 signaling has also been shown to play a critical role in modulating the invasive potential of human pancreatic cancer lines (30) as well as the transition from pancreatic inflammation to pancreatic cancer in genetically-engineered mouse models (31), we sought to determine whether LPS, alone or in combination with IFN-γ, might regulate Duox2-mediated ROS generation in pancreatic cancer cells.

Hence, in this study, we evaluated the effects of IFN-γ and LPS on Duox2 expression and function, as well the mechanism(s) by which these two pro-inflammatory agents regulate Duox2 levels in human pancreatic cancer cell lines. We found that while both agents significantly increase Duox2 expression individually, the combination synergistically enhances the expression of Duox2 and its associated maturation factor, DuoxA2, leading to a significant increase in both extracellular and intracellular ROS production. The dramatic increase in ROS we observed for the combination of LPS and IFN-γ depended critically on the upregulation of and signaling through the TLR4 pathway, ultimately resulting in enhanced binding of NF-κB (p65) to the Duox2 promoter. We also found that ROS

production under our experimental conditions was sufficient to activate the DNA damage repair pathway while arresting cells in G_1, and producing a significant increase in apoptosis as well as inhibition of cellular proliferation. To determine whether Duox2 might contribute to inflammatory states in vivo, we examined its expression both in tissue specimens from patients with chronic pancreatitis and in pancreatic cancer xenografts; in both cases, we found that Duox2 expression levels were markedly up-regulated. These results suggest that the pro-oxidant state generated by cytokine-mediated Duox2 upregulation could hinder recovery from inflammatory stress-related tissue injury and, thus, may contribute to the development and pathologic behavior of pancreatic cancer cells.

Materials and Methods

Materials

Recombinant human IFN-γ (catalog number 285-IF) was from R & D systems. Antibody against human β-actin (catalog number A3853) was acquired from Sigma-Aldrich. Our Stat1 (p84/p91) (sc-346) antibody was obtained from Santa Cruz Biotechnology. Antibodies against components of the nuclear factor–kappa B (NF-κB) complex including p65 (catalog number 6956), IκBα (catalog number 34812), *p*-Stat1(Ser^{727}) (catalog number 9177S), as well as *p*-Stat1(Tyr^{701}) (catalog number 9167L) and *p*-Histone γH2AX (Ser^{139})(catalog number 2577S) were purchased from Cell Signaling Technology. Human TLR4 silencer select siRNA (catalog number 4390825), silencer negative control siRNA (catalog number AM4635), human Duox2 primer (catalog number Hs00204187_m1), human DuoxA2 primer (catalog number Hs01595310_m1), human TLR4 primer (catalog Hs00152939_ml), human MyD88 primer (catalog number Hs00182082_ml), human actin (catalog number Hs99999903_m1), and TaqMan Universal PCR mix (catalog number 4364340) were from Applied Biosystems. The QuikChIP Kit (catalog number 3010K), anti-human TLR4 antibody (catalog number IMG-6307A), anti-human TLR4 FITC antibody, and the Cell Surface TLR Staining Flow Kit (catalog number 10099K) were from Imgenex. 2′,7′-Dichlorodihydrofluorescein diacetate (CM-H_2DCFDA) was obtained from Molecular Probes (Carlsbad, CA). 1-Pyrrolidinecarbodithioic acid, ammonium salt (PDTC) (catalog number 548000) and BAY11-70829 (catalog number 196870) were from EMD Chemicals, Gibbstown, NJ. 3-(4,5-Dimethylthiazol-2-yl)-2,5-diphenyltetrazolium bromide (MTT) (catalog number M2128) was from Sigma-Aldrich. Our mouse anti-human Duox monoclonal antibody, S-12, was developed by Creative Biolabs, Port Jefferson Station, NY and characterized as described previously {Wu, 2011 15660 /id}. Although the pancreatic cancer cell lines utilized for these experiments do not contain measurable Duox1 mRNA, because the antibody cross-reacts with Duox1, we have referred to the protein it detects as “Duox”. The three human pancreas tissue microarrays (BIC14011, PA485, PA1001) were obtained from US Biomax, Inc., Rockville, MD.

Cell lines, cell culture, and mice

The human pancreatic cancer cell lines BxPC-3 (catalog number CRL-1687), AsPC-1 (catalog number CRL-1682), and MIA-PaCa (catalog number CRL-1420) were obtained from the American Type Culture Collection, Manassas, VA. Cells were cultured in RPMI 1640 medium (catalog number SH30255.01; Hyclone) with 1% pyruvate and 10% FBS. CFPAC-1 pancreatic cancer cells (catalog number CRL-1918) were also obtained from the ATCC and were cultured in Iscove's Modified Dulbecco's medium with 10% FBS. The identity of each cell line was confirmed using Identifiler® STR genotyping (Applied Biosystems). For starvation conditions, cells were propagated overnight in the same medium without FBS. We used starvation conditions because, although the induction of Duox2 expression by IFN-γ was observed under both serum-containing and serum-starved conditions, Duox2 induction was stronger after starvation. Cells were cultured in a

humidified incubator at 37 °C in an atmosphere of 5% CO_2 in air. In control experiments, we found that the basal levels of expression of all of the Nox homologues (Nox1-5 and Duox1 and 2) in each of the pancreatic cancer cell lines employed for these studies were very low, often at or near the lower limit of detection of our real time, RT-PCR assays (data not shown). All mice (female athymic nu/nu NCr) used in the study were obtained from the Animal Production Program (Frederick National Laboratory for Cancer Research, Frederick, MD). NCI-Frederick is accredited by AAALAC International and follows the Public Health Service Policy for the Care and Use of Laboratory Animals. Animal care was provided in accordance with the procedures outlined in the "Guide for Care and Use of Laboratory Animals" (National Research Council; 1996; National Academy Press; Washington, D.C.)

RNA extraction, cDNA synthesis, and quantitative real-time RT-PCR assay

Total RNA was extracted from IFN-γ– or LPS-treated or untreated cells with the RNeasy Mini Kit (catalog number 74104; Qiagen) according to the manufacturer's instructions. Two micrograms of total RNA was used for cDNA synthesis, using SuperScript II reverse transcriptase (catalog number 18080-044) and random primers (catalog number 48190-011; Invitrogen) in a 20-μl reaction system, with the following cycles: 25 °C for 5 min, 42 °C for 50 min, and 75 °C for 5 min. After the reaction was complete, the RT-PCR products were diluted with diethylpyrocarbonate/H_2O to 100 μl for real-time PCR. Real-time RT-PCR was performed on 384-well plates in a 20 μl reaction system containing 2 μl of diluted cDNA, 1 μl of primer mixture, 7 μl of H_2O, and 10 μl of TaqMan 2× reaction mixture. PCR was carried out under default cycling conditions, and fluorescence was detected with the ABI 7900HT Sequence Detection System (Applied Biosystems, Foster City, CA). Triplicate determinations were performed for each sample that was used for real-time PCR; the mean value was calculated, and the data in the final figures represent the results of three independent experiments. Relative gene expression was calculated as the ratio of the target gene to the internal reference gene (β-actin) multiplied by 10^6 based on *Ct* values.

Whole-cell and nuclear extract preparation and Western analysis

For preparation of whole-cell extracts, cell pellets from BxPC-3, AsPC-1, and CFPAC-1 cells, treated with or without IFN-γ and/or LPS, were lysed with 1× RIPA Lysis Buffer (catalog number 20-188; Millipore, Temecula, CA), with the addition of a phosphatase inhibitor tablet (catalog number 04-906-837001; Roche) and a protease inhibitor tablet (catalog number 11-836-153001; Roche). The NE-PER Nuclear and Cytoplasmic Extraction Kit (catalog number 78833; Thermo Scientific) was used to prepare nuclear extract from cells treated with IFN-γ and/or LPS. The protein concentrations of both whole-cell and nuclear extracts were measured by using the BCA Protein Assay Kit (Pierce). Cell extracts were mixed with an equal volume of 2× SDS protein gel loading buffer (catalog number 351-082-661; Quality Biological); 50 μg of whole-cell extract was loaded onto a 4–20% Tris glycine gel (catalog number EC6028; Invitrogen), and the proteins were separated and electrophoretically transferred to nitrocellulose membranes using I Blot gel transfer stacks (catalog number IB 3010-01; Invitrogen). The membranes were blocked in 1× TBST buffer with 5% nonfat milk for 1 hr at room temperature and then incubated with primary antibody overnight in TBST buffer. Membranes were washed three times in 1× TBST buffer and incubated with HRP–conjugated secondary antibody for 1 hr at room temperature with shaking. The antigen–antibody complex was visualized with SuperSignal West Pico Luminol/Enhancer Solution (catalog number 1856136, Thermo Scientific). To evaluate Duox2 expression, the whole-cell extract was mixed with an equal volume of 2× SDS loading buffer without boiling; for other proteins, the mixture of cell extract with loading buffer was boiled for 5 min. As previously noted (24), Duox2 aggregates when the whole-cell extract is boiled; the mobility of the Duox2 protein is much slower with boiling than without.

Chromatin immunoprecipitation

Chromatin immunoprecipitation (ChIP) assays to detect the binding of the NF-κB p65 subunit to the Duox2 promoter in vivo were carried out with the QuikChIP Kit (catalog number 30101K; Imgenex) according to the manufacturer's protocol. Starved BxPC-3 cells treated with or without IFN-γ and/or LPS were cross-linked with 1% formaldehyde, and the cross-linking was stopped by the addition of glycine (final concentration of 125 mM) to the medium. Cells were then harvested and resuspended in 1× SDS lysis buffer. The suspended cells were sonicated to produce 200- to 1,000-bp genomic fragments. For immunoprecipitation, NF-κB antibody (catalog number 6956; Cell Signaling Technology) or normal rabbit IgG antibody (Santa Cruz Biotechnology) were used to pull down the cross-linked DNA protein complex. The purified DNA was used as a PCR template to amplify the NF-κB target sequence in the human Duox2 promoter. The primer sequences were as follows: 5′-GAGAGGAGCCAGAAGCAGAA- 3′ and 5′-AGACGGAATCCGGAGAGACT-3′. The resulting PCR products were 221 bp in length.

Measurement of intracellular ROS production by flow cytometry

BxPC-3 cells (1×10^6) primed with solvent or with IFN-γ and/or LPS were suspended in 0.5 ml of Krebs buffer containing 7.5 μM of the redox-sensitive dye CM-H_2-DCF-DA and incubated in the dark for 30 min at 37 °C. After 25 min of incubation, either solvent (DMSO) or 1 μM ionomycin was added to the cell suspension, and the incubation was continued at 37 °C for an additional 5 min. The cells were then harvested and resuspended in fresh medium without CM-H_2-DCF-DA. Fluorescence was recorded on the FL-1 channel of a FACS Aria flow cytometer (BD Bioscience) and analyzed using Flowjo Software (24).

Extracellular H_2O_2 measurement using Amplex Red®

The Amplex Red® Hydrogen Peroxide/Peroxidase Assay Kit (catalog number A22188; Invitrogen) was used to detect extracellular H_2O_2 released by IFN-γ– and/or LPS-activated cells, as previously described (24). BxPC-3 cells were grown in serum-free medium with or without IFN-γ and/or LPS for 24 hr; the cells were then washed twice with 1× PBS, trypsinized, and dispersed thoroughly. Cells were counted to produce a 20-μl cell suspension containing 2×10^4 live BxPC-3 cells in 1× KRPG buffer. The cells were mixed with 100 μl of Amplex Red® reagent containing 50 μM Amplex Red® and 0.1 units of HRP per ml in Krebs-Ringer phosphate glucose (KRPG) buffer with or without 1 μM ionomycin and incubated at 37 °C for 60 min. The fluorescence of the oxidized 10-acetyl-3,7-dihydroxyphenoxazine was measured at an excitation wavelength of 530 nm and an emission wavelength of 590 nM, using a SpectraMax Multiplate reader (Molecular Devices, Sunnyvale, CA). H_2O_2 was quantified with an H_2O_2 standard curve over a 0- to 2-μM concentration range. Each value in the figures represents a mean of quadruplicate samples from 16 readings.

MTT assay for cell proliferation

BxPC-3 or AsPC-1 cells were seeded in 96-well plates at a density of 1×10^4 cells per well in 100 μl of complete medium overnight. The next day medium was changed with solvent, and IFN-γ (25 ng/ml) or LPS (1 μg/ml) or both were added. On days 1 and 2 after treatment, cell proliferation was evaluated by the MTT method. In short, the culture medium was removed and 100 μl of MTT at a concentration of 0.5 mg/ml was added to each well. The plates were then incubated at 37 °C for 45 min. The MTT was then removed, and 100 μl of MTT solvent was added to each well. The plates were shaken for 10 min and read at 570 nM with the plate reader.

Cell cycle progression and measurement of apoptosis by analytical cytometry

Determination of cell cycle progression was performed using a cell cycle analysis kit (cat# L00287, Gen Scrip, Inc.). BxPC-3 cells grown in complete medium were treated with solvent, 1 μg/ml LPS, 25 ng/ml of IFN-γ, or both for 24 h. Cells were then trypsinized, counted, and 1×10^6 cells were washed with 1 × PBS, and fixed with 70% ethanol at 4 °C for at least 2 h, or overnight. The fixation solution was removed, and the cells were washed once again with 1 × PBS. Cells were incubated in 100 μl of RNase at 37 °C for 30 min; then, 400 μl of propidium iodide was added to each sample to stain the cells at 37 °C for an additional 30 min in the dark. Finally, the labeled cells were subjected to analytical cytometry utilizing a BD FACS caliber flow cytometer (BD Biosciences, San Jose, California). Data from experiments performed in triplicate were analyzed with ModFit v3.0 software. For measurement of apoptosis, BxPC-3 cells were propagated in complete medium, and then treated with solvent, 1 μg/ml LPS, 25 ng/ml of IFN-γ, or both for 72 h. Cells were trypsinized and counted; both dead and live cells were collected for our apoptosis assay which used the Vybrant Apoptosis Assay Kit #3 (Invitrogen, cat# V13242) with a 7-AAD viability staining solution (Biolegend, cat# 420404). Cell labeling was carried out according to the Manufacturer's protocol; in brief, 1×10^5 cells were suspended in 100 μl of 1X annexin binding buffer to which was added 5 μl of FITC annexin 5 and 2 μl of 7-AAD viability staining solution. The cells were incubated at room temperature in the dark for 15 min; at the end of that time, 400 μl of annexin binding buffer was added. The stained cells were analyzed with a BD FACS caliber flow cytometer as soon as possible thereafter. Data were analyzed with Flowjo software.

Tumor growth, propagation, and sampling

Human pancreatic tumor cells for mouse inoculation were used at the 4^{th} to 6^{th} in vitro passage from cryopreserved cell stocks. Cells (1×10^7 cells/0.1 ml/injection) were subcutaneously inoculated bilaterally into mice (n = 20 mice per tumor cell line). This provided a total of 40 potential tumor samples. Two groups were prepared by randomization on the day of inoculation; 10 mice each were placed into 300 mg and 500 mg tumor harvest groups. When tumors reached the target size, they were resected, cut into quadrants, and flash frozen. Flash freezing was accomplished by placing the tumor quadrants into prechilled cryovials followed by immediate submersion into liquid nitrogen. All samples were transferred to a -70 °C freezer for holding prior to processing. For the current experiments, the 300 mg BxPC-3 and the 500 mg AsPC-1 and MIA-PaCa tumors were studied. NCI-Frederick is accredited by AAALACi and follows the Public Health Service Policy on the Care and Use of Laboratory Animals. All animals used in this research project were cared for and used humanely according to the following policies: The U.S. Public Health Service Policy on Humane Care and Use of Animals (1996); the Guide for the Care and Use of Laboratory Animals Eighth Edition; and the U.S. Government Principles for Utilization and Care of Vertebrate Animals Used in Testing, Research, and Training (1985).

RNA and protein extraction from tumor xenografts

In addition to the methods described for cell lines above, a Polytron System PT 1200E homogenizer equipped with a 5-12 mm diameter dispersing head (KINEMATICA AG, Switzerland) was used to homogenize the tumor tissue mixed with a suitable amount of either 1 X RIPA buffer for protein extraction or RLT buffer for RNA extraction. A 350 μl volume of tumor homogenate was processed directly for isolation of RNA. For protein lysate preparation, the tumor homogenate in RIPA buffer was centrifuged at 13000 rpm and 4 °C for 10 min; the supernatant was used for Western analysis and to determine protein concentration.

Immunohistochemical analysis of Duox expression in pancreatic tissue arrays from patients with chronic pancreatitis

Immunohistochemistry using our Duox monoclonal antibody was performed on three human pancreatic tissue microarrays. Immunohistochemistry staining was performed as follows: slides were deparaffinized with distilled water; antigen retrieval was performed using DAKO target retrieval solution (#S1699) for 20 min at 95 °C followed by 20 min of cooling. Slides were rinsed in distilled water, transferred to TBST buffer (DAKO #S3006) for 5 min, and incubated in peroxidase blocking solution (3% H_2O_2) for 10 min at room temperature (RT). Duox antibody at a dilution of 1:250 (diluted in DAKO diluent #S0809) was used for 60 min at RT; slides were then rinsed in TBST and secondary antibody was applied (DAKO EnVision+ Dual Link System-HRP [#K4063], Ready-To-Use) for 30 min at RT. The slides were rinsed in TBST (3 times, 2 min each); DAB (3,3′-diaminobenzidine) was used for 10 min for visualization, and the slides were rinsed in TBST. Hematoxylin was used as a counterstain. Positive control tissues (normal human colon and cell pellets) and a negative control reagent (normal mouse IgG1 isotype control 10 μg/ml for 60 min [BD Biosciences #550878], diluted in DAKO diluent #S0809) were also examined.

Statistical analysis

Results are expressed as the mean ± standard deviation from at least triplicate experiments. Statistical differences between mean values of control and treated samples were assessed using Student's *t* test; $p < 0.05$ was considered statistically significant. Significance levels were designated as * = $p < 0.05$, ** = $p < 0.01$, and *** = $p < 0.001$ throughout.

Results

Combination of LPS and IFN-γ synergistically induces Duox2 expression and reactive oxygen production

BxPC-3 cells were treated with IFN-γ and/or LPS to determine the potential of each, as well as the combination, to induce Duox2 expression. LPS alone significantly increased Duox2 mRNA levels in BxPC-3 cells, albeit to a lesser degree than IFN-γ; however, the combination of LPS and IFN-γ increased Duox2 expression ≈ 6-fold compared to IFN-γ alone, $p < 0.001$ (Fig. 1*A*, upper panel). In control experiments, we found that decreasing the LPS concentration to 100 ng/ml did not alter the synergistic induction of Duox2 expression with IFN-γ that we observed; Duox2 rather than Duox1 was the predominant oxidase affected by the combination of IFN-γ and LPS (Supplemental Fig. 3). Western analysis confirmed that LPS- and IFN-γ–induced Duox2 mRNA expression correlated well with Duox protein levels (Fig. 1*A*, lower panel). The simultaneous exposure of cells to both LPS and IFN-γ induced a substantially higher level of Duox protein expression than either LPS or IFN-γ (Fig. 1*A*). In like manner (Fig. 1*B*), we found that the addition of LPS to IFN-γ significantly increased the expression of the Duox2 maturation factor, DuoxA2, that plays a critical role in the formation of the active Duox2 membrane oxidase (32). To determine whether these levels of Duox2 and DuoxA2 correlated with functional oxidase activity, we examined the production of reactive oxygen species (ROS) using two different techniques. In the presence of 1 μM ionomycin for 1 h, which is known to activate Duox 2 (13), BxPC-3 cells previously exposed for 24 h to IFN-γ and/or LPS produced significant amounts of extracellular H_2O_2 (Fig. 1*C*) as detected with the Amplex Red® reagent; co-treatment with LPS and IFN-γ resulted in significantly more extracellular H_2O_2 production than exposure to either agent alone. To confirm our results obtained with Amplex Red®, we performed flow cytometric quantitation of intracellular ROS production using the redox-sensitive dye CM-H_2-DCF-DA. These studies clearly demonstrated that intracellular ROS levels were increased following exposure of BxPC-3 cells to LPS and/or IFN-γ; and that the ROS levels observed were consistent with the expression levels of Duox2 and DuoxA2 following

exposure to LPS or IFN-γ, alone or in combination (Fig. 1*D*). Whereas intracellular ROS production in BxPC-3 cells following ionomycin treatment was modestly increased by LPS itself, and was increased to a greater degree by IFN-γ, exposure to the combination of LPS and IFN-γ resulted in substantially greater ROS production than did exposure to either agent alone (Fig. 1*D*). Finally, we found that ionomycin-enhanced H_2O_2 production by BxPC-3 cells exposed to LPS and IFN-γ could be significantly decreased following pretreatment with Duox2-specific siRNA (Fig. 1*E*). Taken together, these data are consistent with the synergistic induction of functional Duox2 and DuoxA2 by the combination of LPS and IFN-γ.

IFN-γ and LPS upregulate TLR4 and MyD88 in association with enhanced Duox2 expression levels

It has been reported previously that exposure to IFN-γ augments the expression of TLR4 and its accessory components, MD-2 and MyD88, in human monocytes and macrophages (33). In those experiments, exposure of IFN-γ–primed monocytes to LPS enhanced the phosphorylation of IL-1 receptor–associated kinase, NFκB DNA binding activity, and TNF-α and IL-12 production. Furthermore, Abreu and colleagues reported that intestinal epithelial cells expressed low levels of TLR4 and MD-2 and were hypo-responsive to LPS; however, in the same cells, the pro-inflammatory cytokines IFN-γ and TNF-α increased TLR4 and MD-2 expression and sensitized epithelial cells to LPS-dependent IL-8 secretion (34). We sought to determine whether our observed synergistic induction of Duox2 by LPS and IFN-γ occurred by the same mechanism. We used real-time RT-PCR to evaluate the expression of TLR4 and its adaptor protein MyD88 after exposure of BxPC-3 cells to solvent, LPS, and/or IFN-γ. IFN-γ induced a significant, approximately three- to four-fold increase in TLR4 and MyD88 expression in BxPC-3 cells, and the combination of LPS and IFN-γ increased TLR4, but not MyD88, levels further (Fig. 2*A*). Western analysis confirmed that the increase in IFN-γ–induced TLR4 and MyD88 mRNA correlated with an increase in protein expression; we also found, as previously described (24), that treatment of BxPC-3 cells with IFN-γ enhanced the phosphorylation of Stat1 at tyrosine 701 (Fig. 2*B*). Finally, we evaluated the surface expression of TLR4 after IFN-γ exposure by flow cytometry using an FITC-labeled human TLR4 antibody. BxPC-3 cells demonstrated expression of TLR4 on the cell surface that was enhanced by IFN-γ, resulting in a substantial right shift of the fluorescent signal (Fig. 2*C*).

Silencing of TLR4 attenuated IFN-γ– and LPS-mediated induction of TLR4 and Duox2/DuoxA2 expression

We used RNA interference to further define the role of TLR4 in the synergistic induction of Duox2 and DuoxA2 by LPS and IFN-γ in BxPC-3 cells. Control siRNA or two distinct human TLR4-specific siRNAs targeting different domains of TLR4 were transiently transfected into BxPC-3 cells. At 24 h following transfection, cells were cultured in serum-free medium with LPS and/or IFN-γ for another 24 h. Cells were then collected and subjected to RNA extraction and real-time RT-PCR. Human TLR4 siRNAs were found to specifically suppress IFN-γ– and LPS-induced TLR4 expression (Fig. 3*A*) but had no inhibitory effect on IFN-γ–induced Stat1 expression (Fig. 3*B*). Human TLR4 siRNAs also significantly attenuated the expression of IFN-γ– and LPS-induced Duox2 (Fig. 3*C*) and DuoxA2 (Fig. 3*D*), whereas control siRNAs had no inhibitory effect on the expression of IFN-γ– and LPS-induced TLR4, or Duox2/DuoxA2. Western analysis confirmed that TLR4 siRNA had an inhibitory effect on LPS- and IFN-γ–induced TLR4 protein expression (Fig. 3*E*). Silencing of TLR4 also decreased LPS- and IFN-γ–induced Duox protein expression (Fig. 3*E*, lanes 4 and 8).

Intact NF-κB signaling is required for LPS- and IFN-γ–induced Duox2 expression

To expand our results with BxPC-3 cells, the AsPC-1 human pancreatic cancer cell line was also exposed to IFN-γ; as demonstrated in Fig. 4*A*, these cells also respond to IFN-γ by increasing the expression of Duox2. We sought, as well, to determine whether LPS and IFN-γ act synergistically to induce Duox2 expression in AsPC-1 cells as they do in the BxPC-3 line. Starved AsPC-1 cells were treated with solvent or with LPS (1 μg/ml) and/or IFN-γ (25 ng/ml), and real-time RT-PCR was used to evaluate TLR4 and Duox2 expression. Although treatment of AsPC-1 cells with IFN-γ alone induced a significant level of Duox2 expression, in marked contrast to our results in BxPC-3 cells, exposure to LPS as well as IFN-γ did not result in a further significant increase in Duox2 expression (Fig. 4*A*). Furthermore, IFN-γ, either alone or in combination with LPS, increased TLR4 expression by approximately four-fold over the levels observed with solvent or LPS (Fig. 4*B*). Whole-cell extracts from AsPC-1 cells that had been treated for 24 h with LPS and/or IFN-γ were subjected to Western analysis. As shown in Fig. 4*D*, IFN-γ activated Stat1 signaling in this cell line and augmented Duox expression. IFN-γ treatment also induced TLR4 expression, but unlike BxPC-3 cells, co-treatment with LPS did not result in a further increase in Duox protein levels. We next compared NF-κB signaling in the two cell lines after priming the cells with either solvent or IFN-γ for 24 h and then exposing the cells to LPS for 1 h. In BxPC-3 cells, priming the cells with IFN-γ and treating for 1 h with LPS resulted in IκBα degradation (Fig. 4*C*; compare lanes 1 and 4). In contrast, for AsPC-1 cells, exposure to LPS plus IFN-γ did not result in IκBβ degradation (Fig. 4*E*). Finally, we examined nuclear extracts prepared from BxPC-3 and AsPC-1 cells that had been primed with either solvent or IFN-γ for 24 h and then treated with LPS for 1 h. In both cell lines, IFN-γ priming resulted in a similar level of nuclear accumulation of Stat1 and interferon regulatory factor–1 (IRF-1) (Fig. 4*F*), which was not dependent on LPS treatment. Results for the transcription factor NF-κB, however, differed in the two cell lines. In BxPC-3 cells, LPS exposure alone resulted in a clear nuclear translocation of NF-κB; priming with IFN-γ prior to treatment with LPS resulted in further enhancement of the nuclear accumulation of NF-κB. However, in AsPC-1 cells, the nuclear distribution of NF-κB was not influenced by either LPS or IFN-γ treatment (Fig. 4*F*). To evaluate the generality of our finding that NF-κB signaling could play an important role in regulating the expression of Duox2 in human pancreatic cancer cells, we also evaluated the effects of IFN-γ and LPS on CFPAC-1 human pancreatic cancer cells (Supplemental Fig. 1). In this line, similar to our observations with BxPC-3 cells, we found that exposure to IFN-γ and LPS produced a more than additive effect on Duox2 expression at both the RNA and protein levels that was accompanied by activation of TLR4 and was associated with degradation of IκBα (Supplemental Fig. 1*A,B,C*). Furthermore, nuclear accumulation of NF-κB following LPS and IFN-γ exposure resembled our findings in BxPC-3, and not in AsPC-1 cells (Supplemental Fig. 2). These results suggest that an intact NF-κB signaling pathway is necessary for the synergistic induction of Duox2 by LPS and IFN-γ in human pancreatic cancer cells.

Inhibition of NF-κB diminished LPS- and IFN-γ–induced Duox2 expression in BxPC-3 cells

To investigate further whether LPS- and IFN-γ–mediated induction of Duox2 depended on NF-κB activation, we exposed BxPC-3 cells to two different NF-κB inhibitors, pyrrolidine dithiocarbamate (PDTC; 100 μM) and BAY 11-7082 (10 μM), for 30 min prior to LPS and/or IFN-γ. Both inhibitors significantly decreased LPS- and IFN-γ–mediated Duox2 induction (Fig. 5*A*), indicating that activation of NF-κB is required for Duox2 induction by LPS and IFN-γ. Neither NF-κB inhibitor over the time course and concentrations tested was cytotoxic, as measured by exclusion of trypan blue dye (data not shown).

NF-κB p65 binds to the human Duox2 promoter

Having confirmed that IFN-γ exposure can upregulate TLR4 and MyD88 expression in BxPC-3 cells, and is associated with a more than additive effect on Duox2 expression when combined with LPS, as well as accumulation of NF-κB p65 in the nucleus, we sought to determine whether a component of the NF-κB complex could bind to the human Duox2 promoter. We also wished to examine whether such binding would be enhanced by co-treatment with LPS and IFN-γ over that seen with either LPS or IFN-γ treatment alone. Chromatin immunoprecipitation (ChIP) was used to investigate binding of the NF-κB p65 subunit in vivo under various experimental conditions. Using the TRANSFAC® search program (35), we identified a canonical NF-κB binding site within 3 kb of the human Duox2 promoter between -2771 to -2763 bp from the transcription start site. The sequence was 5′-GGGAATTCCC-3′, which exactly matched the known NF-κB consensus motif (5′-GGGRNNTYCC-3′) provided by TRANSFAC®. PCR primers were therefore designed on the basis of the DNA sequence surrounding the potential NF-κB binding site. Equal amounts of DNA were used for the initial immunoprecipitation (Fig. 5*B*, top panel). Control IgG antibody produced a very weak background PCR signal, indicating immunoprecipitation, and that PCR reactions were specific (Fig. 5*B*, middle panel). With a p65-specific antibody (Fig. 5*B*, bottom panel), LPS and IFN-γ treatment produced a clear PCR product; co-treatment with LPS and IFN-γ, furthermore, produced a much stronger PCR signal that was indicative of greater p65 binding to the endogenous human Duox2 promoter.

LPS and IFN-γ treatment leads to extracellular H_2O_2 accumulation, inhibition of growth and cell cycle progression, and induction of apoptosis and DNA damage in human pancreatic cancer cells

To examine potential consequences of LPS- and IFN-γ-mediated upregulation of Duox2 and DuoxA2, we examined the time course of extracellular H_2O_2 accumulation following a variety of stimulation conditions. Surprisingly, in the absence of ionomycin stimulation, extracellular H_2O_2 production by BxPC-3 cells steadily increased over time; after 4 h of incubation, extracellular H_2O_2 production for cells that had been exposed for 24 h previously to IFN-γ or the combination of LPS plus IFN-γ continued to generate H_2O_2 at substantial levels (Fig. 6*A*). When ionomycin was added to the reaction system, the differences among the treatment conditions became more pronounced (Fig. 6*B*); cells primed with LPS plus IFN-γ produced the highest amounts of extracellular H_2O_2, consistent with their expression levels of Duox2 and DuoxA2. On the other hand, consistent with the lower levels of Duox2 expression measured in AsPC-1 cells following treatment with IFN-γ and/or LPS, the production of H_2O_2 was lower in these cells (Fig. 6*C*) and was enhanced to a much lesser degree by the presence of the calcium ionophore (Fig. 6*D*). We next measured the effects of LPS and IFN-γ on cell growth in BxPC-3 and AsPC-1 cells, using the MTT assay (Fig. 6*E* and *F*). On day 1, there was no significant difference among the various treatment groups. On day 2, LPS alone still demonstrated no inhibitory effect on cell proliferation; in contrast, IFN-γ alone significantly inhibited the growth of BxPC-3 cells. The combination of LPS and IFN-γ resulted in >50% retardation of cell growth by day 2 of exposure. In comparison, IFN-γ induces both Duox2 and DuoxA2 expression in AsPC-1 cells to a lesser degree than for the BxPC-3 line; neither IFN-γ, alone or combined with LPS, had an inhibitory effect on AsPC-1 cell growth (Fig. 6*F*). These data suggest that the sustained intra- and extracellular ROS production mediated by LPS- and IFN-γ-induced Duox2 expression in BxPC-3 cells may be sufficient (at least when compared to the AsPC-1 line) to affect tumor cell proliferation. To evaluate potential mechanisms of cell death, we examined the effects of IFN-γ and LPS on cell cycle progression and apoptosis in BxPC-3 cells. As shown in Fig. 7*A*, exposure of BxPC-3 cells to IFN-γ and LPS produced a profound inhibition of cell cycle progression at G_1 that exceeded that of IFN-γ alone, and which is consistent with an effect of H_2O_2 (36); the G_1 arrest was associated with a marked

degree of both apoptotic cell death and loss of cell membrane permeability (Fig. 7*B*). Finally, to examine the possibility that Duox2-related reactive oxygen metabolism might contribute to enhanced genetic instability of our pancreatic cancer cells, we evaluated the effect of IFN-γ and LPS on the activation of phosphorylated γH2AX, a biomarker for DNA damage and repair (37). As shown in Fig. 7*C*, we found that both IFN-γ alone or the IFN-γ and LPS combination induced a marked DNA damage response in BxPC-3 cells. Furthermore, the γH2AX signal was decreased by pretreatment of the BxPC-3 cells with either the ROS scavenger N-acetyl-L-cysteine or by a formulation of the H_2O_2 detoxifying enzyme catalase (PEG-catalase) that crosses the tumor cell outer membrane. These studies indicate that ROS produced by IFN-γ in combination with LPS may produce DNA damage that activates a DNA repair response measurable by the expression of γH2AX.

Growth of human pancreatic cancer cells as xenografts is associated with increased Duox2 expression

In our current experiments, as well as our previous study (24), we found that Duox2 expression in human pancreatic cancer cells in culture is very low in the absence of cytokine exposure; and certain pancreatic lines, MIA-PaCa cells for example, are unresponsive to IFN-γ. We hypothesized that it might be possible to evaluate the relevance of our current investigations to the setting of tumor cell growth in vivo by examining whether the extracellular milieu of pancreatic tumor cells growing as xenografts could provide an environment that was sufficiently pro-inflammatory to alter Duox2 expression in the absence of treatment with an exogenous cytokine. As shown in Fig. 8, we found that during the first passage of BxPC-3 or AsPC-1 cells in athymic mice, when tumors reached 300 to 500 mg in size, respectively, Duox2 expression increased dramatically, compared to the expression levels in the cells immediately prior to xenografting. Furthermore, for both the BxPC-3 and AsPC-1 lines, Duox2 expression in vivo approximated that following exposure to IFN-γ for 24 h in vitro (Fig. 8*A* and *B*, upper panels). On the other hand, the level of Duox2 in MIA-PaCa cells—which is at the lower limit of detection by RT-PCR and which does not respond to IFN-γ—did not change following growth of the tumor in vivo as a xenograft (Fig. 8*C*, upper panel). Tumors of 500 mg, rather than 300 mg, were used to study the AsPC-1 and MIA-PaCa xenografts to optimize the chance for upregulation of Duox2. Western analysis from lysates prepared from the same tumors (that had been split into quarters) used for RT-PCR, confirmed the changes in expression that we found at the mRNA level (Fig. 8*A,B,C* lower panels).

Duox expression is increased in patients with chronic pancreatitis

To evaluate the expression of Duox earlier in the process of pancreatic carcinogenesis, we performed immunohistochemical analyses using three different human pancreatic tissue arrays that included normal pancreatic tissue from 10 patients (18 spots), and chronic pancreatitis specimens from 48 patients (49 spots). The specimens of normal pancreas had a low level, diffuse, cytoplasmic signal which was most noticeable within pancreatic islets (Fig. 9*A*). None of the normal pancreas specimens had evidence of membrane staining. The majority of the pancreatitis specimens (34/48) had multifocal, markedly increased Duox staining in both cytoplasm and membrane that was most noticeable in duct(ule)s (Fig. 9*B*). Minimal inflammation and low numbers of ducts, as well as sampling variability, was considered the probable reason for negative results in some of the pancreatitis cases (data not shown). Increased staining in patients with pancreatitis was often closely associated with areas of inflammatory cell infiltrates (Fig. 10).

Discussion

Oxidative stress plays a critical role in modulating the innate immune response to inflammatory stimuli (38,39). Further, there is increasing evidence that the source of at least some of the ROS that accompany acute and chronic inflammation in many organs is one or more epithelial members of the Nox family of oxidases (in addition to the Nox2 found in granulocytes and macrophages) (3,4,40). Thus, in the experiments reported here, we sought to evaluate in pancreatic cancer cells the mechanism(s) by which pro-inflammatory stimuli regulate the expression of Duox2, the Nox family member that supplies a substantive amount of the H_2O_2 utilized for host defense by airway mucosal cells as well as organs of the gastrointestinal tract (17,41).

In a previous study, we demonstrated that IFN-γ upregulated both Duox2, and its critical maturation factor DuoxA2, in a Stat1-dependent fashion which involved both the Jak and p38-MAPK pathways (24). Specific binding of Stat1 to the Duox2 promoter plays an essential role in the up-regulation of Duox2 in BxPC-3 human pancreatic cancer cells, and the subsequent Duox2-related production of a substantive flux of H_2O_2. It has been observed that pancreatic cancer lines, like certain other epithelial tumors, express TLRs (30), and are capable of signal transduction through TLR-related pathways previously thought to be an exclusive characteristic of immune cells (42). Furthermore, Ochi and colleagues recently reported that LPS accelerates tumorigenesis in the pancreas and that inhibition of TLR4 signaling significantly decreased the development of inflammation-related pancreatic tumors in vivo (31). These studies support our evaluation of the effect of LPS alone and in combination with IFN-γ on the formation of ROS by cancer cells of pancreatic origin as well as our examination of Duox2 expression during the growth of pancreatic tumor models in vivo and in the process of pancreatic inflammation in man.

We found that the combination of IFN-γ and LPS produced a substantially greater than additive effect on Duox2 expression in BxPC-3 (Fig. 1) and CFPAC-1 (Supplemental Fig. 1), but not AsPC-1 (Fig. 4) pancreatic cancer cells. The major increase in expression of Duox2 and DuoxA2 that we observed was accompanied by a significant enhancement of functional oxidase activity measured by extracellular H_2O_2 formation and intracellular ROS production (Fig. 1). Although IFN-γ increased the expression of activated Stat1 to a similar degree in all three cell lines, the addition of LPS did not lead to any further change in Duox2 levels in AsPC-1 cells when compared to the BxPC-3 and CFPAC-1 lines (Fig. 4).

The divergent responses of these cell lines to co-treatment with LPS and IFN-γ prompted us to examine the underlying mechanisms that might explain these differences. Under baseline conditions, NF-κB is sequestered in the cytoplasm by the inhibitory activity of IκBα. The engagement of LPS to the TLR4 receptor results in the activation of IκB kinases (IKKs). Activated IKKs phosphorylate IκBα, leading to its ubiquitination and subsequent degradation. Once IκBα is degraded, NF-κB is released and translocates to the nucleus where it can bind to DNA sequences known as κB sites, resulting in the transcriptional activation of many inflammation-related genes (43). A critical role for the NF-κB pathway in the explanation of our findings is supported by the observation that pre-treatment with inhibitors of NF-κB signaling, PDTC and BAY117082, significantly decreased Duox2 expression following exposure to IFN-γ and LPS (Fig. 5*A*). Furthermore, as shown in Fig. 4 and Supplemental Fig. 2, following IFN-γ priming, exposure to LPS in BxPC-3 and CFPAC-1 cells leads to degradation of IκBα and substantial translocation of NF-κB (p65) to the nucleus, whereas translocation of NF-κB (p65) to the nucleus is minimal in AsPC-1 cells under the same experimental conditions. It seems likely that this major difference in activation of NF-κB signaling may help to explain the absence of LPS-related enhancement

of Duox2/DuoxA2 expression in the AsPC-1 line (Fig. 4*D*) versus that observed for BxPC-1 and CFPAC-1 cells.

The requirement for upregulation of TLR4-related signaling in the control of Duox2 expression by IFN-γ and LPS was substantiated by the RNA interference studies shown in Fig. 3; siRNAs targeting different sites on TLR4 not only decreased TLR4 expression but decreased Duox2 and DuoxA2 expression at the RNA level, as well as the expression of Duox protein, without altering the increase in activated Stat1 levels that we observed previously following exposure to IFN-γ alone (24). These results are consistent with prior studies demonstrating that LPS-induced reactive oxygen production in the THP-1 human monocyte line required TLR4-mediated signaling through the NF-κB pathway (44); and that in HEK293 cells that express Nox4, a direct interaction between TLR4 and the Nox4 isoform is required to sustain LPS-mediated ROS generation and activation of NF-κB (25). Our finding that exposure of BxPC-3 cells to IFN-γ and LPS leads to enhanced binding of NF-κB (p65) to the Duox2 promoter strongly suggests that two concomitant mechanisms interact to produce the marked increase in Duox2 expression we observed (Fig. 1). LPS alone enhances p65 binding to the Duox2 promoter; the combination of LPS and IFN-γ increases p65 binding further. In complementary fashion, IFN-γ by itself appears to increase Duox2 expression by increasing the binding of Stat1 to the Duox2 promoter (24). We suggest that the combined transcriptional activation produced by p65 and Stat1 are responsible for the dramatic increase in Duox2 expression and function observed in these experiments.

Cytokine-induced Duox2 expression in BxPC-3 cells also significantly increased extracellular H_2O_2 production in the presence or absence of stimulation by ionomycin (Fig. 6). The H_2O_2 levels produced were of sufficient magnitude to decrease the proliferation of BxPC-3 cells by ≈ 50% (Fig. 6*E*); decreased tumor cell growth was associated with a significant block in the G_1 phase of the cell cycle and markedly enhanced apoptosis (Fig. 7*A,B*). On the other hand, H_2O_2 production in the AsPC-1 line, which upregulates Duox2 following IFN-γ treatment to a lesser degree than BxPC-3 cells, was only modestly changed under these conditions (Fig. 6*D*) and was not associated with any change in proliferation. Exposure to IFN-γ and LPS also produced DNA double strand breaks (as measured by an increase in phosphorylated γH2AX) in BxPC-3 cells that could be diminished by ROS scavengers (Fig. 7*C*). This degree of oxidant stress is consistent with a role for Duox2-mediated ROS in producing LPS-dependent injury to the extracellular matrix (30) as well as contributing to tumor cell genomic instability. These results also support recent studies suggesting that increased Duox2 expression in the intestinal epithelial cells of patients with Crohn's disease and ulcerative colitis may have pathophysiologic significance (21).

We recently demonstrated that Duox2 can be highly expressed in human colorectal cancers in comparison with adjacent normal colonic tissue (14). Other investigators have reported a 10-fold increase in Duox2 expression in pre-malignant adenomatous polyps in the large intestine compared to adjacent normal tissue in the same individuals (45), further supporting a role for Duox2 in malignant transformation. A role for Duox2 in both human pancreatic cancer and chronic pancreatitis is supported by our in vivo experiments demonstrating the rapid upregulation of Duox2 expression in two human tumor cell lines (BxPC-3 and AsPC-1) grown as xenografts, but not for an IFN-γ-unresponsive line (MIA PaCa cells), as well as the increased staining for Duox in patients with chronic pancreatitis (Figs. 9 and 10). Our results are concordant with an investigation by Fukushima and associates that found Duox2 expression to be increased 13.6-fold in tissue adjacent to infiltrating pancreatic ductal carcinomas evaluated by mRNA expression array analysis (46).

Finally, it is important to note that chronic pancreatic inflammation, in addition to being a pre-malignant condition, can result in inflammation-related pancreatic fibrosis which can produce severe clinical consequences (1,2). Recent studies suggest that in model systems inflammation can be interrupted by treatment with inhibitors of the Nox gene family, leading to the prevention of many of the ROS-related morphologic consequences of chronic inflammation in the pancreas (3).

In summary, our experiments demonstrate that the pro-inflammatory stimuli IFN-γ and LPS significantly enhance the transcription of Duox2 and DuoxA2 leading to the production of substantial amounts of extracellular H_2O_2 by human pancreatic cancer cell lines, and that H_2O_2 generation may depend on the activation of both Stat1 and NF-κB signaling pathways. Furthermore, expression of Duox appears to be increased in human pancreatic cancer models in vivo and in chronic pancreatitis in man. In light of these data, support exists for the possibility that Duox2-related H_2O_2 production could provide an oxidative local milieu that would enhance leukocyte recruitment, increase genetic instability, and that is sufficiently pro-angiogenic to be conducive to malignant transformation (9,47,48). Our ongoing studies are focused on how an understanding of the pathophysiologic consequences of increased Duox2 expression in pancreatic cancer could lead to novel methods to interrupt pro-inflammatory cycles of oxidative injury in the gastrointestinal tract.

Supplementary Material

Refer to Web version on PubMed Central for supplementary material.

Acknowledgments

This work was supported by the Center for Cancer Research and the Division of Cancer Treatment and Diagnosis, National Cancer Institute, National Institutes of Health; the work was also conducted, in part, under Contract No. HHSN261200800001E. The content of this publication does not necessarily reflect the views or policies of the Department of Health and Human Services, nor does mention of trade names, commercial products, or organizations imply endorsement by the U.S. Government.

References

1. Farrow B, Evers BM. Inflammation and the development of pancreatic cancer. Surg. Oncol. 2002; 10:153–169. [PubMed: 12020670]
2. Greer JB, Whitcomb DC. Inflammation and pancreatic cancer: an evidence-based review. Curr. Opin. Pharmacol. 2009; 9:411–418. [PubMed: 19589727]
3. Masamune A, Watanabe T, Kikuta K, Satoh K, Shimosegawa T. NADPH oxidase plays a crucial role in the activation of pancreatic stellate cells. Am. J. Physiol. Gastrointest. Liver Physiol. 2008; 294:G99–G108. [PubMed: 17962358]
4. Yu JH, Lim JW, Kim H, Kim KH. NADPH oxidase mediates interleukin-6 expression in cerulein-stimulated pancreatic acinar cells. Int. J. Biochem. Cell Biol. 2005; 37:1458–1469. [PubMed: 15833277]
5. Guerra C, Collado M, Navas C, Schuhmacher AJ, Hernandez-Porras I, Canamero M, Rodriguez-Justo M, Serrano M, Barbacid M. Pancreatitis-induced inflammation contributes to pancreatic cancer by inhibiting oncogene-induced senescence. Cancer Cell. 2011; 19:728–739. [PubMed: 21665147]
6. Vaquero EC, Edderkaoui M, Pandol SJ, Gukovsky I, Gukovskaya AS. Reactive oxygen species produced by NAD(P)H oxidase inhibit apoptosis in pancreatic cancer cells. J. Biol. Chem. 2004; 279:34643–34654. [PubMed: 15155719]
7. Edderkaoui M, Hong P, Vaquero EC, Lee JK, Fischer L, Friess H, Buchler MW, Lerch MM, Pandol SJ, Gukovskaya AS. Extracellular matrix stimulates reactive oxygen species production and increases pancreatic cancer cell survival through 5-lipoxygenase and NADPH oxidase. Am. J. Physiol. Gastrointest. Liver Physiol. 2005; 289:G1137–G1147. [PubMed: 16037546]

8. Mochizuki T, Furuta S, Mitsushita J, Shang WH, Ito M, Yokoo Y, Yamaura M, Ishizone S, Nakayama J, Konagai A, Hirose K, Kiyosawa K, Kamata T. Inhibition of NADPH oxidase 4 activates apoptosis via the AKT/apoptosis signal-regulating kinase 1 pathway in pancreatic cancer PANC-1 cells. Oncogene. 2006; 25:3699–3707. [PubMed: 16532036]
9. Chiera F, Meccia E, Degan P, Aquilina G, Pietraforte D, Minetti M, Lambeth D, Bignami M. Overexpression of human NOX1 complex induces genome instability in mammalian cells. Free Radic. Biol. Med. 2008; 44:332–342. [PubMed: 17963706]
10. Driessens N, Versteyhe S, Ghaddhab C, Burniat A, De Deken X, Van Sande J, Dumont JE, Miot F, Corvilain B. Hydrogen peroxide induces DNA single- and double-strand breaks in thyroid cells and is therefore a potential mutagen for this organ. Endocrine-Related Cancer. 2009; 16:845–856. [PubMed: 19509065]
11. Ostman A, Hellberg C, Bohmer FD. Protein-tyrosine phosphatases and cancer. Nat. Rev. Cancer. 2006; 6:307–320. [PubMed: 16557282]
12. Szatrowski TP, Nathan CF. Production of large amounts of hydrogen peroxide by human tumor cells. Cancer Res. 1991; 51:794–798. [PubMed: 1846317]
13. Bedard K, Krause KH. The NOX family of ROS-generating NADPH oxidases: physiology and pathophysiology. Physiol. Rev. 2007; 87:245–313. [PubMed: 17237347]
14. Juhasz A, Ge Y, Markel S, Chiu A, Matsumoto L, van Balgooy J, Roy K, Doroshow JH. Expression of NADPH oxidase homologues and accessory genes in human cancer cell lines, tumours and adjacent normal tissues. Free Radic. Res. 2009; 43:523–532. [PubMed: 19431059]
15. Caillou B, Dupuy C, Lacroix L, Nocera M, Talbot M, Ohayon R, Deme D, Bidart JM, Schlumberger M, Virion A. Expression of reduced nicotinamide adenine dinucleotide phosphate oxidase (ThoX, LNOX, Duox) genes and proteins in human thyroid tissues. J. Clin. Endocrinol. Metab. 2001; 86:3351–3358. [PubMed: 11443211]
16. Harper RW, Xu C, Eiserich JP, Chen Y, Kao CY, Thai P, Setiadi H, Wu R. Differential regulation of dual NADPH oxidases/peroxidases, Duox1 and Duox2, by Th1 and Th2 cytokines in respiratory tract epithelium. FEBS Lett. 2005; 579:4911–4917. [PubMed: 16111680]
17. El Hassani RA, Benfares N, Caillou B, Talbot M, Sabourin JC, Belotte V, Morand S, Gnidehou S, Agnandji D, Ohayon R, Kaniewski J, Noel-Hudson MS, Bidart JM, Schlumberger M, Virion A, Dupuy C. Dual oxidase2 is expressed all along the digestive tract. Am. J. Physiol. Gastrointest. Liver Physiol. 2005; 288:G933–G942. [PubMed: 15591162]
18. Allaoui A, Botteaux A, Dumont JE, Hoste C, De Deken X. Dual oxidases and hydrogen peroxide in a complex dialogue between host mucosae and bacteria. Trends Molec. Med. 2009; 15:571–579. [PubMed: 19913458]
19. Geiszt M, Witta J, Baffi J, Lekstrom K, Leto TL. Dual oxidases represent novel hydrogen peroxide sources supporting mucosal surface host defense. Faseb J. 2003; 17:1502–1504. [PubMed: 12824283]
20. Gattas MV, Forteza R, Fragoso MA, Fregien N, Salas P, Salathe M, Conner GE. Oxidative epithelial host defense is regulated by infectious and inflammatory stimuli. Free Radic. Biol. Med. 2009; 47:1450–1458. [PubMed: 19703552]
21. Lipinski S, Till A, Sina C, Arlt A, Grasberger H, Schreiber S, Rosenstiel P. DUOX2-derived reactive oxygen species are effectors of NOD2-mediated antibacterial responses. J. Cell Sci. 2009; 122:3522–3530. [PubMed: 19759286]
22. Ha EM, Lee KA, Seo YY, Kim SH, Lim JH, Oh BH, Kim J, Lee WJ. Coordination of multiple dual oxidase-regulatory pathways in responses to commensal and infectious microbes in drosophila gut. Nat. Immunol. 2009; 10:949–957. [PubMed: 19668222]
23. Csillag C, Nielsen OH, Vainer B, Olsen J, Dieckgraefe BK, Hendel J, Vind I, Dupuy C, Nielsen FC, Borup R. Expression of the genes dual oxidase 2, lipocalin 2 and regenerating islet-derived 1 alpha in Crohn's disease. Scand. J. Gastroenterol. 2007; 42:454–463. [PubMed: 17454855]
24. Wu Y, Antony S, Juhasz A, Lu J, Ge Y, Jiang G, Roy K, Doroshow JH. Up-regulation and sustained activation of Stat1 are essential for interferon-gamma (IFN-gamma)-induced dual oxidase 2 (Duox2) and dual oxidase A2 (DuoxA2) expression in human pancreatic cancer cell lines. J. Biol. Chem. 2011; 286:12245–12256. [PubMed: 21321110]

25. Park HS, Jung HY, Park EY, Kim J, Lee WJ, Bae YS. Cutting edge: direct interaction of TLR4 with NAD(P)H oxidase 4 isozyme is essential for lipopolysaccharide-induced production of reactive oxygen species and activation of NF-kappa B. J. Immunol. 2004; 173:3589–3593. [PubMed: 15356101]
26. Ogier-Denis E, Mkaddem SB, Vandewalle A. NOX enzymes and Toll-like receptor signaling. Semin. Immunopathol. 2008; 30:291–300. [PubMed: 18493762]
27. Testro AG, Visvanathan K. Toll-like receptors and their role in gastrointestinal disease. J. Gastroenterol. Hepatol. 2009; 24:943–954. [PubMed: 19638078]
28. Zhang X, Zhu C, Wu D, Jiang X. Possible role of toll-like receptor 4 in acute pancreatitis. Pancreas. 2010; 39:819–824. [PubMed: 20664479]
29. Sharif R, Dawra R, Wasiluk K, Phillips P, Dudeja V, Kurt-Jones E, Finberg R, Saluja A. Impact of toll-like receptor 4 on the severity of acute pancreatitis and pancreatitis-associated lung injury in mice. Gut. 2009; 58:813–819. [PubMed: 19201771]
30. Ikebe M, Kitaura Y, Nakamura M, Tanaka H, Yamasaki A, Nagai S, Wada J, Yanai K, Koga K, Sato N, Kubo M, Tanaka M, Onishi H, Katano M. Lipopolysaccharide (LPS) increases the invasive ability of pancreatic cancer cells through the TLR4/MyD88 signaling pathway. J. Surg. Oncol. 2009; 100:725–731. [PubMed: 19722233]
31. Ochi A, Nguyen AH, Bedrosian AS, Mushlin HM, Zarbakhsh S, Barilla R, Zambirinis CP, Fallon NC, Rehman A, Pylayeva-Gupta Y, Badar S, Hajdu CH, Frey AB, Bar-Sagi D, Miller G. MyD88 inhibition amplifies dendritic cell capacity to promote pancreatic carcinogenesis via Th2 cells. J. Exp. Med. 2012; 209:1671–1687. [PubMed: 22908323]
32. Grasberger H, Refetoff S. Identification of the maturation factor for dual oxidase. Evolution of an eukaryotic operon equivalent. J. Biol Chem. 2006; 281:18269–18272. [PubMed: 16651268]
33. Bosisio D, Polentarutti N, Sironi M, Bernasconi S, Miyake K, Webb GR, Martin MU, Mantovani A, Muzio M. Stimulation of toll-like receptor 4 expression in human mononuclear phagocytes by interferon-gamma: a molecular basis for priming and synergism with bacterial lipopolysaccharide. Blood. 2002; 99:3427–3431. [PubMed: 11964313]
34. Abreu MT, Arnold ET, Thomas LS, Gonsky R, Zhou Y, Hu B, Arditi M. TLR4 and MD-2 expression is regulated by immune-mediated signals in human intestinal epithelial cells. J. Biol. Chem. 2002; 277:20431–20437. [PubMed: 11923281]
35. Quandt K, Frech K, Karas H, Wingender E, Werner T. MatInd and MatInspector: new fast and versatile tools for detection of consensus matches in nucleotide sequence data. Nucleic Acids Res. 1995; 23:4878–4884. [PubMed: 8532532]
36. Chen QM, Bartholomew JC, Campisi J, Acosta M, Reagan JD, Ames BN. Molecular analysis of H2O2-induced senescent-like growth arrest in normal human fibroblasts: p53 and Rb control G1 arrest but not cell replication. Biochem. J. 1998; 332(Pt 1):43–50. [PubMed: 9576849]
37. Redon CE, Nakamura AJ, Zhang YW, Ji JJ, Bonner WM, Kinders RJ, Parchment RE, Doroshow JH, Pommier Y. Histone gammaH2AX and poly(ADP-ribose) as clinical pharmacodynamic biomarkers. Clin. Cancer Res. 2010; 16:4532–4542. [PubMed: 20823146]
38. Kolls JK. Oxidative stress in sepsis: a redox redux. J. Clin. Invest. 2006; 116:860–863. [PubMed: 16585954]
39. Yu M, Lam J, Rada B, Leto TL, Levine SJ. Double-stranded RNA induces shedding of the 34-kDa soluble TNFR1 from human airway epithelial cells via TLR3-TRIF-RIP1-dependent signaling: roles for dual oxidase 2- and caspase-dependent pathways. J. Immunol. 2011; 186:1180–1188. [PubMed: 21148036]
40. Rada B, Leto TL. Characterization of hydrogen peroxide production by Duox in bronchial epithelial cells exposed to Pseudomonas aeruginosa. FEBS Lett. 2010; 584:917–922. [PubMed: 20085766]
41. Nagai K, Betsuyaku T, Suzuki M, Nasuhara Y, Kaga K, Kondo S, Nishimura M. Dual Oxidase 1 and 2 Expression in Airway Epithelium of Smokers and Patients with Mild/Moderate Chronic Obstructive Pulmonary Disease. Antioxid. Redox Signal. 2008; 10:705–714. [PubMed: 18177232]
42. Chen R, Alvero AB, Silasi DA, Steffensen KD, Mor G. Cancers take their Toll--the function and regulation of Toll-like receptors in cancer cells. Oncogene. 2008; 27:225–233. [PubMed: 18176604]

43. Gloire G, Legrand-Poels S, Piette J. NF-kappaB activation by reactive oxygen species: fifteen years later. Biochem. Pharmacol. 2006; 72:1493–1505. [PubMed: 16723122]
44. Ryan KA, Smith MF Jr. Sanders MK, Ernst PB. Reactive oxygen and nitrogen species differentially regulate Toll-like receptor 4-mediated activation of NF-kappa B and interleukin-8 expression. Infect. Immun. 2004; 72:2123–2130. [PubMed: 15039334]
45. Kita H, Hikichi Y, Hikami K, Tsuneyama K, Cui ZG, Osawa H, Ohnishi H, Mutoh H, Hoshino H, Bowlus CL, Yamamoto H, Sugano K. Differential gene expression between flat adenoma and normal mucosa in the colon in a microarray analysis. J. Gastroenterol. 2006; 41:1053–1063. [PubMed: 17160516]
46. Fukushima N, Koopmann J, Sato N, Prasad N, Carvalho R, Leach SD, Hruban RH, Goggins M. Gene expression alterations in the non-neoplastic parenchyma adjacent to infiltrating pancreatic ductal adenocarcinoma. Mod. Pathol. 2005; 18:779–787. [PubMed: 15791284]
47. Niethammer P, Grabher C, Look AT, Mitchison TJ. A tissue-scale gradient of hydrogen peroxide mediates rapid wound detection in zebrafish. Nature. 2009; 459:996–999. [PubMed: 19494811]
48. Arbiser JL, Petros J, Klafter R, Govindajaran B, McLaughlin ER, Brown LF, Cohen C, Moses M, Kilroy S, Arnold RS, Lambeth JD. Reactive oxygen generated by Nox1 triggers the angiogenic switch. Proc. Natl. Acad. Sci. USA. 2002; 99:715–720. [PubMed: 11805326]

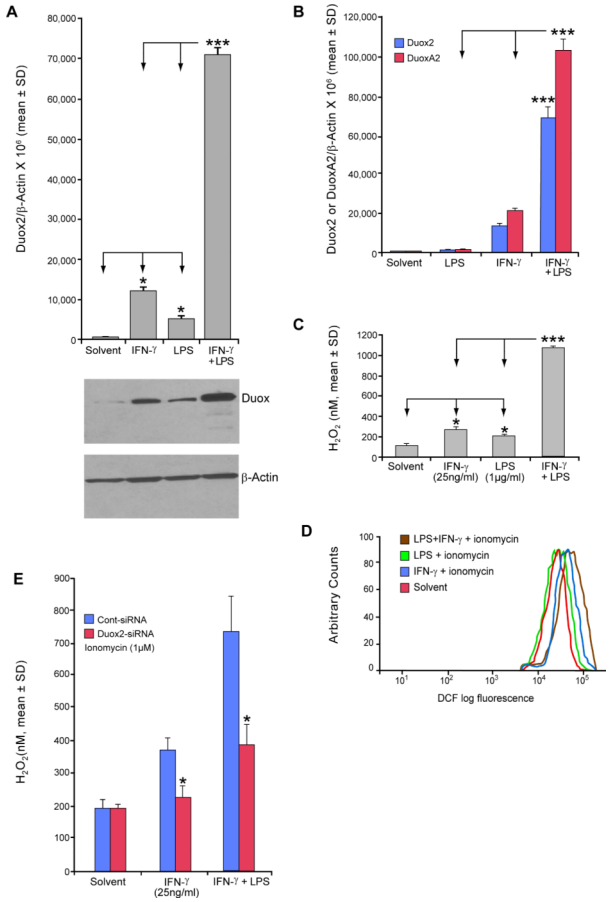

FIGURE 1.

LPS acts synergistically with IFN-γ to induce Duox2 and DuoxA2 expression, enhancing both intra- and extracellular production of ROS. *A*, The upper panel demonstrates the induction of Duox2 expression by exposure to IFN-γ (25 ng/ml), LPS (1 μg/ml), or the combination for 24 h; quantitative, real-time RT-PCR analysis of relative Duox2 expression has been normalized to β-actin; error bars represent standard deviations; data are from triplicate experiments; * = $p < 0.05$ for the comparison of Duox2 expression in either IFN-γ- or LPS-treated BxPC-3 cells and solvent-treated controls; *** = $p < 0.001$ for the comparison between the combination of LPS and IFN-γ pretreatment versus either agent alone. The lower panel demonstrates the expression of the Duox protein by Western analysis in 50 μg of whole cell extract from BxPC-3 cells treated with solvent, IFN-γ (25 ng/ml), LPS (1 μg/ml), or both IFN-γ and LPS for 24 h; the Western blot shown is representative of three independent experiments. *B*, The expression of both Duox2 and DuoxA2 following treatment with IFN-γ (25 ng/ml), LPS (1 μg/ml), or the combination for 24 h was quantitated by real-time RT-PCR normalized to β-actin; error bars represent standard deviations; data represent the means of three independent experiments; *** = $p < 0.001$ for the comparison between the combination of LPS and IFN-γ pretreatment versus either agent alone for both Duox2 and DuoxA2. *C*, Extracellular H_2O_2 production was detected using the Amplex Red® hydrogen peroxide/peroxidase assay. BxPC-3 cells were grown in serum-free medium with IFN-γ and/or LPS for 24 h. Cells were then collected, and 2×10^4 live BxPC-3 cells were mixed with 100 μl of the Amplex Red® reaction mixture containing 50 μM Amplex Red® and 0.1 U of HRP per ml of Krebs-Ringer phosphate buffer with 1 μM ionomycin for 1 h. H_2O_2 values were calculated by interpolation from a standard curve, using 0–2 μM H_2O_2. Data are shown as means ± SD; $n = 16$; * = $p < 0.05$ for the

comparison between IFN-γ or LPS pretreatment and solvent; *** = $p < 0.001$ for the comparison between the combination of IFN-γ and LPS and either agent used independently. *D*, Production of intracellular ROS by IFN-γ- and/or LPS-treated BxPC-3 pancreatic carcinoma cells as detected by flow cytometry. Starved BxPC-3 cells were treated with solvent, IFN-γ (25 ng/ml), LPS (1 μg/ml), or both IFN-γ and LPS for 24 h; intracellular ROS production was measured at the end of the incubation by FACS, using the redox-sensitive dye CM-H_2-DCF-DA. Ionomycin (1 μM) was added for 5 min following completion of IFN-γ and/or LPS treatment, prior to resuspension of the cells in fresh medium and quantitation of fluorescence. The figure shown is representative of three independent experiments. *E*, Effect of Duox2 siRNA on ionomycin-enhanced extracellular H_2O_2 production in BxPC-3 cells pretreated with IFN-γ or the combination of IFN-γ and LPS. The cells were treated with IFN-γ, or IFN-γ and LPS, and H_2O_2 production was quantitated with ionomycin exposure exactly as described in panel *C* above, except that 24 h prior to exposure to IFN-γ or IFN-γ and LPS, control siRNA or siRNA targeting Duox2 were transfected into BxPC-3 cells. Data are shown as means ± SD; $n = 3$, * = $p < 0.05$ for the comparison between IFN-γ or IFN-γ and LPS pretreatment following transient transfection with either control or Duox2 siRNA.

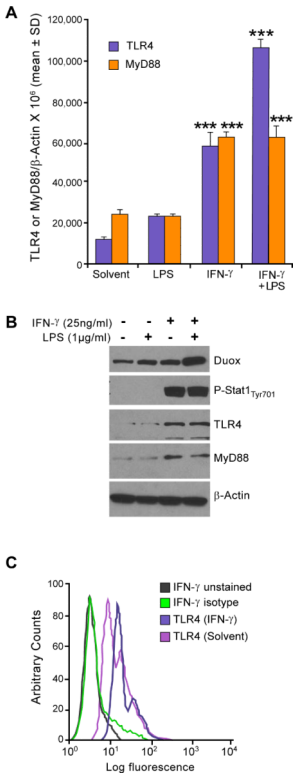

FIGURE 2.

Enhanced TLR-4 expression is associated with LPS- and IFN-γ–mediated increases in Duox2/DuoxA2 levels in BxPC-3 cells. *A*, BxPC-3 cells were grown in serum-free medium and treated with IFN-γ (25 ng/ml) or LPS (1 μg/ml) or both for 24 h. RNA was then extracted and subjected to real-time RT-PCR to evaluate TLR4/MyD88 expression normalized to β-actin; error bars represent standard deviations; data are from triplicate experiments (nine readings); *** = $p < 0.001$ versus solvent alone. *B*, Fifty micrograms of whole cell extract from BxPC-3 cells was treated with solvent or exposed to IFN-γ (25 ng/ml), LPS (1 μg/ml), or both for 24 h and then subjected to Western analysis with TLR4, MyD88, phospho-Stat1, and Stat1-specific antibodies. Data shown are representative of three independent experiments. *C*, IFN-γ–induced cell surface expression of TLR4 was detected by analytical cytometry. Starved BxPC-3 cells were treated with solvent or IFN-γ (25 ng/ml) for 24 h and then stained with either FITC-conjugated isotype control or human TLR4-specific antibody; labeled cells were then analyzed by flow cytometry; the figure shown is an example taken from three separate experiments.

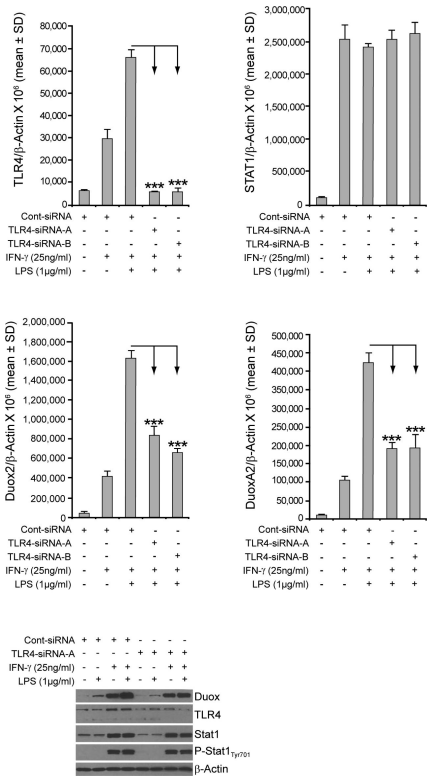

FIGURE 3.

Silencing TLR4 attenuates IFN-γ– and LPS-mediated enhancement of TLR4 and Duox2/DuoxA2 expression in BxPC-3 cells. *A*, Inhibition of TLR4 expression by TLR4 siRNAs. Control siRNA or two human TLR4-specific siRNAs targeting different domains of TLR4 were transiently transfected into BxPC-3 cells; 24 h following transfection, cells were incubated in serum-free medium with or without IFN-γ (25 ng/ml) or LPS (1 μg/ml) for another 24 h. RNA was then extracted and subjected to real-time RT-PCR, and relative TLR4 levels were normalized to β-actin. Error bars represent standard deviations; data are from triplicate samples; *** = $p < 0.001$ versus BxPC-3 cells treated with a control siRNA. *B*, Silencing TLR4 produced no effect on IFN-γ–induced Stat1 expression. The identical RNA samples employed in panel *A* were subjected to real-time RT-PCR assay with human Stat1-specific primers, and Stat1 expression relative to β-actin was calculated. *C*, Silencing of TLR4 attenuated IFN-γ– and LPS-induced Duox2 expression. The same RNA samples used for the experiments shown in panel *A* were subjected to real-time RT-PCR using human Duox2-specific primers, and Duox2 expression relative to β-actin was calculated; *** = $p < 0.001$ versus BxPC-3 cells treated with a control siRNA. *D*, Silencing TLR4 attenuated IFN-γ– and LPS-induced DuoxA2 expression. The RNA samples employed for the experiments shown in panel *A* were subjected to real-time RT-PCR assay, using human DuoxA2 primers; DuoxA2 expression relative to β-actin was calculated; *** = $p < 0.001$ versus BxPC-3 cells treated with a control siRNA. *E*, Control or TLR4-specific siRNAs were transiently transfected into BxPC-3 cells. At 24 h after transfection, cells were incubated in serum-free medium with or without IFN-γ (25 ng/ml) or LPS (1 μg/ml) for a subsequent 24 h, and 50 μg of whole cell extract was subjected to Western analysis, using specific antibodies as indicated. These results are representative of three separate experiments.

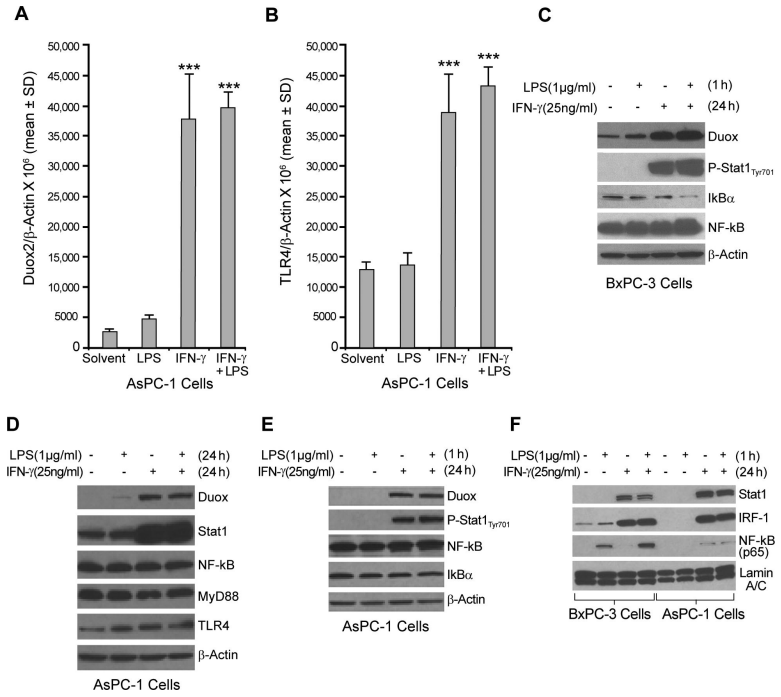

FIGURE 4.

LPS does not enhance IFN-γ–induced Duox2 expression in AsPC-1 human pancreatic cancer cells. *A*, Starved AsPC-1 cells were treated with IFN-γ (25 ng/ml) or LPS (1 μg/ml) for 24 h; 2 μg of total RNA was subjected to real time RT-PCR, and Duox2 expression relative to β-actin was determined; error bars represent standard deviations; data are from triplicate samples; *** = $p < 0.001$ versus AsPC-1 cells treated with solvent. *B*, TLR4 expression was determined using real-time RT-PCR with the same RNA as shown in panel *A*. Human TLR4-specific primers were used for PCR; *** = $p < 0.001$ versus AsPC-1 cells treated with solvent. *C*, LPS activated the NF-κB signaling pathway in BxPC-3 cells. BxPC-3 cells grown in serum-free medium were treated with solvent or IFN-γ (25 ng/ml) for 24 h and then incubated with or without LPS (1 μg/ml) for 1 h; 50 μg of whole cell extract was subjected to Western analysis. These experiments were performed in triplicate. *D*, LPS did not enhance IFN-γ–mediated Duox2 expression in AsPC-1 cells. Starved AsPC-1 cells were treated with IFN-γ (25 ng/ml) or LPS (1 μg/ml) for 24 h, and 50 μg of whole cell extract was subjected to Western analysis, using specific antibodies as indicated. The results are representative of triplicate experiments. *E*, LPS did not activate the NF-κB signaling pathway in AsPC-1 cells. AsPC-1 cells grown in serum-free medium were treated with solvent or IFN-γ (25 ng/ml) for 24 h and then incubated with or without LPS (1 μg/ml) for 1 h; 50 μg of whole cell extract was then subjected to Western analysis. The data shown are representative of three identical experiments. *F*, Effect of LPS on p65 nuclear accumulation in BxPC-3 and AsPC-1 cells exposed to IFN-γ. BxPC-3 and AsPC-1 cells were treated as described in panel *A*, and 20 μg of nuclear extract was subjected to Western analysis to determine Stat1, IRF-1, and p65 distribution in the nucleus. Lamin A/C was used as a loading control for nuclear protein. The data are representative of experiments performed in triplicate.

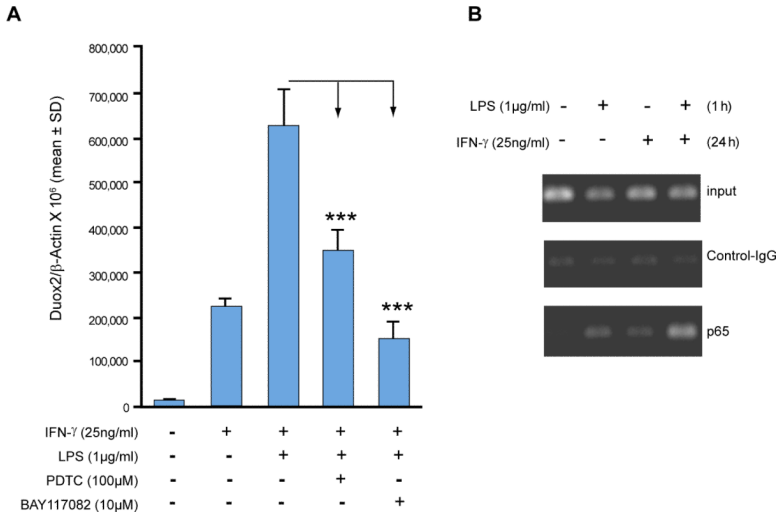

FIGURE 5.

Two independent NF-κB inhibitors attenuate LPS-mediated enhancement of Duox2 expression in IFN-γ–primed BxPC-3 cells and chromatin immunoprecipitation detects binding of NF-κB p65 to the Duox2 promoter in BxPC-3 cells. *A*, BxPC-3 cells were grown in serum-free medium and pretreated with DMSO as the vehicle, or with the NF-κB inhibitors PDTC (100 μM) or BAY 11-7082 (10 μM) for 30 min. Cells were then stimulated with IFN-γ (25 ng/ml) or LPS (1 μg/ml) for 24 h, and RNA was extracted and subjected to real-time RT-PCR to determine Duox2 expression relative to β-actin; *** = $p < 0.001$ versus IFN-γ and LPS exposure without inhibitor pretreatment. Error bars represent standard deviations; data are from triplicate experiments (nine readings for each experimental condition). *B*, ChIP assay detects NF-κB p65 binding to the Duox2 promoter. Starved BxPC-3 cells were treated with solvent or IFN-γ (25 ng/ml) for 24 h and then exposed to LPS (1 μg/ml) for 1 h. Cells were then harvested and used for chromatin immunoprecipitation. Input lanes verify that equal amounts of DNA were used for the initial immunoprecipitation. Control IgG- and p65-specific antibodies were used to pull down DNA, which was then extracted and used for PCR with primers spanning the potential NF-κB binding site in the Duox2 promoter. The resulting PCR products were separated on a 2% agarose gel and visualized with ethidium bromide staining. The experiment was performed in triplicate.

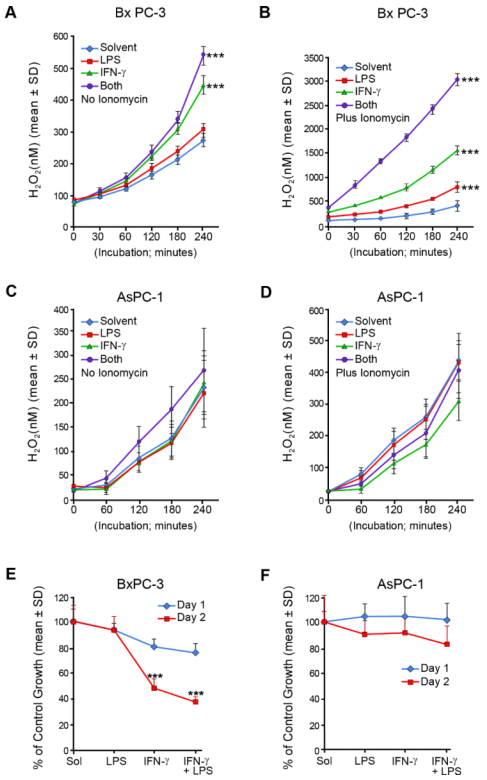

FIGURE 6.

Comparison of the effects of IFN-γ and LPS on extracellular H_2O_2 production and cell growth inhibition in BxPC-3 and AsPC-1 pancreatic cancer cells. Extracellular H_2O_2 was detected using the Amplex Red® assay. BxPC-3 or AsPC-1 cells were grown in serum-free medium treated with solvent, LPS (1 μg/ml), IFN-γ (25 ng/ml), or both LPS and IFN-γ for 24 h. The Amplex Red® assay was then conducted as described in Fig. 1*C* for both BxPC-3 and AsPC-1 cells to detect extracellular H_2O_2 production at different times. *A*, Reaction buffer contained DMSO as the vehicle. H_2O_2 was measured for 4 h in the four experimental groups; the data are expressed as the means ± SD for multiple independent experiments where n=16 for each time point evaluated; *** = $p < 0.001$ versus cells exposed to vehicle alone. *B*, Inclusion of 1 μM ionomycin in the reaction buffer resulted in enhanced H_2O_2 generation. Data are from multiple experiments and are expressed as means ± SD; n = 16; *** = $p < 0.001$ versus cells exposed to vehicle alone. *C*, H_2O_2 production by AsPC-1 cells was determined exactly as described for the BxPC-3 line in the absence of added ionomycin. The data shown are mean values from multiple determinations, n=16. *D*, H_2O_2 production by AsPC-1 cells was examined as described in Fig. 1*C* in the presence of 1 μM ionomycin; the data represent multiple experiments with n=16. *E*, Cell growth was inhibited by exposure to IFN-γ and the combination of IFN-γ and LPS in BxPC-3 cells. BxPC-3 cells grown in serum-free medium were treated with solvent, LPS (1 μg/ml), IFN-γ (25 ng/ml), or both LPS and IFN-γ for 1 or 2 days. MTT assays were then used to evaluate cell proliferation. Data are expressed as means ± SD for multiple experiments; n = 16; *** = $p < 0.001$ versus cells exposed to vehicle alone. *F*, Neither IFN-γ alone or the combination of IFN-γ and LPS significantly inhibited cell growth in the AsPC-1 cell line under experimental conditions identical to those utilized for BxPC-3 cells.

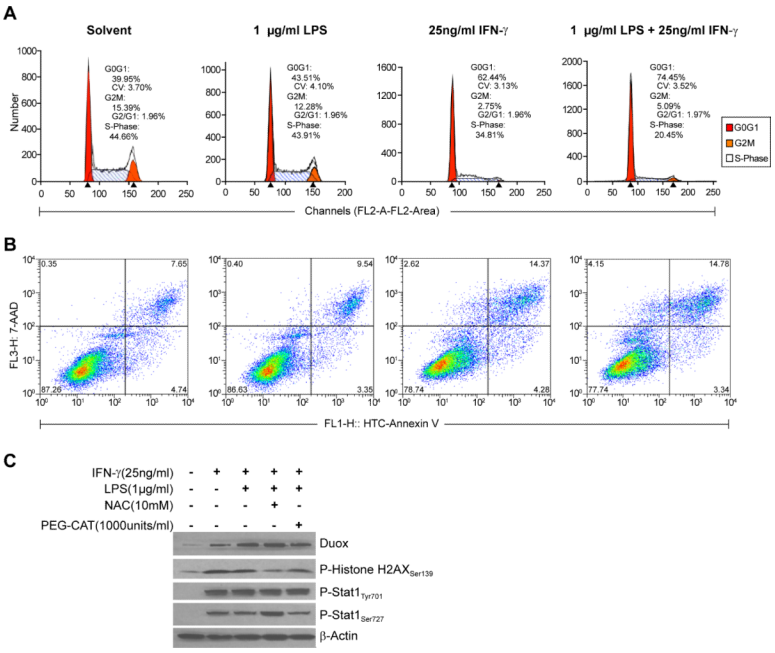

FIGURE 7.

Effects of IFN-γ, LPS, or the combination of IFN-γ and LPS on cell cycle progression, apoptosis, and DNA damage in BxPC-3 cells. *A*, BxPC-3 cells that had been grown in complete media were treated with solvent, LPS (1 μg/ml), IFN-γ (25 ng/ml), or both agents for 24 h. Cells were collected, fixed with 70 % ethanol, stained with propidium iodide, and subjected to analytical cytometry. The data were analyzed with ModFit LT software. *B*, To examine the effects of LPS and/or IFN-γ on cell death in the BxPC-3 line, cells were exposed to each agent individually and in combination for 72 h; live and dead (floating) cells were collected for estimation of the degree of apoptosis utilizing the Vybrant Apoptosis Kit #3 with 7-AAD viability staining solution; labeled cells were analyzed by flow cytometry. Dead cells that cannot exclude 7-AAD were detected in the far red spectral range, depicted on the y-axis; apoptotic cells labeled with FITC conjugated to annexin V are shown with green fluorescence on the x-axis. *C*, IFN-γ and LPS produce DNA double strand breaks in BxPC-3 cells detected by an increase in phosphorylated γH2AX protein. Cells were treated with IFN-γ or the combination of IFN-γ and LPS for 72 h; the thiol-containing ROS scavenger N-acetyl-L-cysteine (NAC) or the cell-permeable H_2O_2-detoxifying enzyme PEG-catalase were administered 30 min prior to the initiation of IFN-γ or IFN-γ plus LPS exposure to evaluate the effect of scavenging ROS on the DNA damage response. Western analysis was performed with 50 μg of cell lysate using the specific antibodies as indicated. The results shown are typical of three identical experiments.

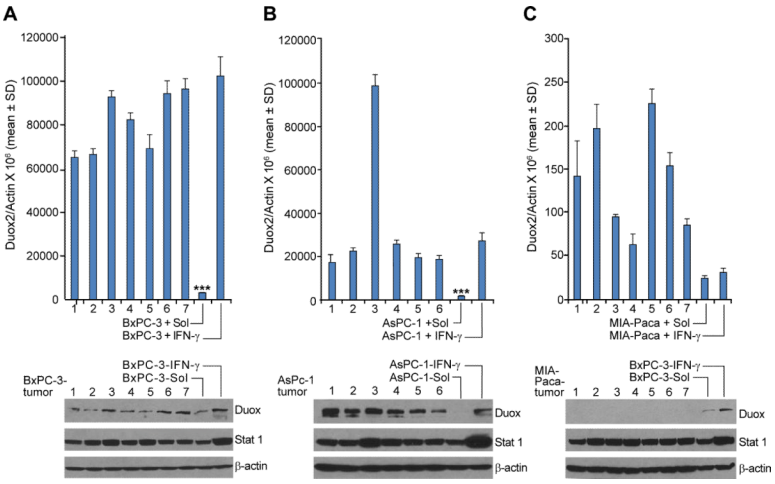

FIGURE 8.

A single in vivo passage as a tumor xenograft significantly increases the expression of Duox2 in BxPC-3 and AsPC-1 but not MIA-PaCa pancreatic cancer cells. BxPC-3, AsPC-1, and MIA-PaCa cells were grown as human tumor xenografts directly from cultured cell lines as described in the 'Materials and Methods' section. *A* and *B*, upper panels, for both BxPC-3 and AsPC-1 cells, Duox2 expression was significantly higher in tumor xenografts than in either cell line examined by real time RT-PCR immediately prior to implantation; *** = $p < 0.001$ for the comparison of pretreatment Duox2 levels in BxPC-3 or AsPC-1 cells in tissue culture either to xenografts or to cells exposed to 25 ng/ml IFN-γ in culture for 24 h; n=6 or 7 individual xenografts for AsPC-1 or BxPC-3 cells, respectively; lower panels, Western analysis confirmed the increase in Duox expression for the individual tumors. *C*, Duox2 expression examined by RT-PCR in MIA-PaCa cells is at the lower limit of detection of our assay; 24 h exposure to IFN-γ (25 ng/ml) in culture cannot therefore be said to change Duox2 levels; furthermore, based on C_t values, Duox2 levels in MIA-PaCa cell xenografts are also at the lower limit of detection of our assay. Duox expression at the protein level could not be demonstrated for MIA-PaCa cells grown as xenografts; lysates from BxPC-3 cells were used as simultaneously-evaluated positive controls.

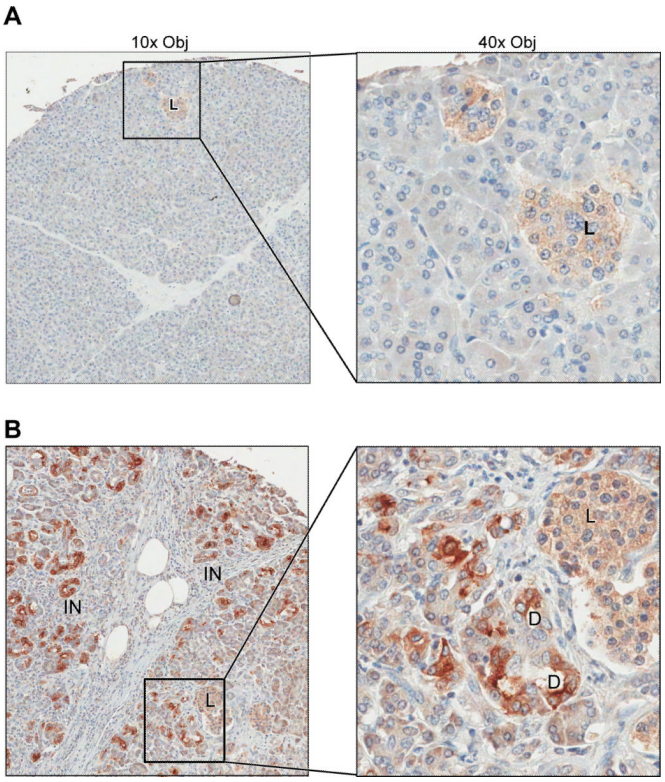

FIGURE 9.

Immunohistochemical analysis demonstrates increased expression of Duox in patients with chronic pancreatitis. *A*, Normal human pancreas. Low level, diffuse, cytoplasmic expression of Duox (light brown stippling) was most noticeable in islets. This diffuse background staining was routinely observed in samples evaluated from 10 patients. *B*, Human pancreas with pancreatitis. Duox expression was increased with notable membrane as well as cytoplasmic staining, particularly in ductal structures. Similar, increased intensity of cytoplasmic and membrane staining for Duox was present in 34 of 48 cases of pancreatitis on the tissue microarrays evaluated. D – ductule; L – islet; IN – inflammation.

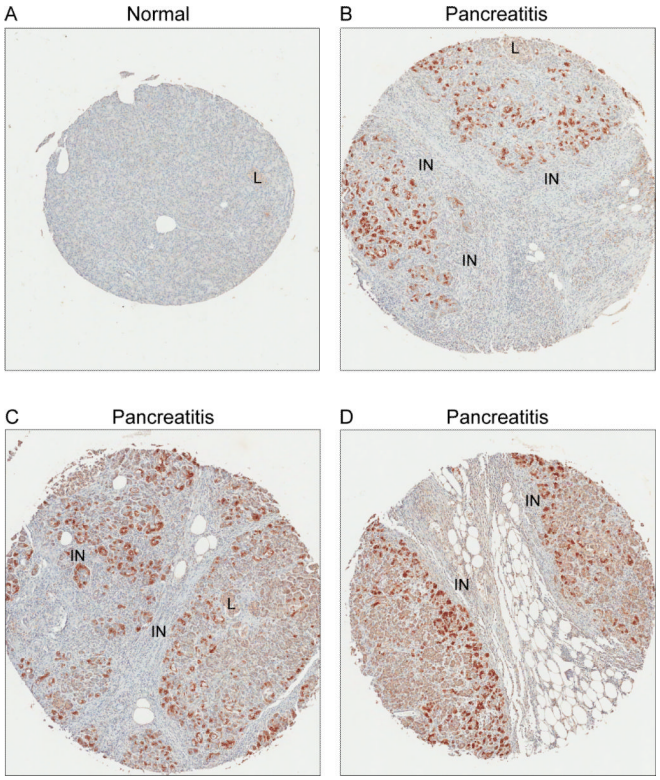

FIGURE 10.

Increased expression of Duox in human cases of pancreatitis is associated with areas of inflammation. *A*, Normal human pancreas. Minimal staining evident by immunohistochemistry. *B-D*, Three different cases of pancreatitis. Increased staining intensity is multifocal with propensity towards areas of inflammatory cell infiltration. Initial magnification, 5x; variation in size of spots is due to different sized microarrays (48 versus 100 spots). L – islet; IN – inflammation.